



A daily gridded dataset of the Fire Weather Index across

2 Canada, with calculations based on the sun's elevation

- 3 Clémence Benoit¹, Jonathan Durand¹, Philippe Gachon^{1,2}, Jonathan Boucher³ and Yan
- 4 Boulanger³

30

- ¹ESCER (Étude et Simulation du Climat à l'Échelle Régionale) Centre, University of Québec at Montréal
- 6 (UQAM), Québec, Canada
- 7 ²Department of Geography, UQAM
- 8 ³Natural Resources Canada, Canadian Forest Service, Québec, Canada
- 9 Correspondence to: Clémence Benoît (benoit.clemence@uqam.ca)
- 10 Abstract. This article summarizes the work carried out at the ESCER (Étude et Simulation du Climat à l'Échelle 11 Régionale, UQAM) Centre to develop the ERA5-FWI-SN dataset - a new automated, gridded dataset of the 12 Canadian Forest Fire Weather Index (FWI) System components for Canada, at a spatial resolution of 13 approximately 31 km. The ERA5-FWI-SN dataset is derived from the hourly ERA5 reanalysis using a new 14 method, called the solar noon method, which is based on the sun's elevation above the local horizon at noon. This 15 method aims to improve the conventional method for calculating the FWI System components, the UTC method, based on the maximum insolation defined via time zones (or specific areas covered by one Coordinated Universal 16 Time zone, i.e. UTC zone), which can cover a wide longitudinal region where the same time prevails. The classical 17 18 method relies on the principle that the average solar time over the territory covered by the same time zone is not 19 too far from legal time (i.e., solar noon is not too far from legal noon), which can be problematic in regions that 20 are very extensive in longitude, such as in Canada where only six time zones have been defined over more than 21 95° of longitudes. The solar noon method also allows for the correction of systematic biases associated with the 22 UTC method, particularly those arising in gridded datasets near time zone boundaries or across the east-west 23 extent of a single time zone. The dataset spans from 1950 to the present and is updated daily through an automation 24 process that allows the calculation of the FWI components with a six-day lag, corresponding to the latest ERA5 25 available reanalysis data for download, resulting in a rapid (i.e., 6-days lag) monitoring of recent wildfire danger 26 throughout Canada. Data were compared between solar noon and UTC methods and were tested against the 27 Canadian Wildland Fire Information System (CWFIS) FWI calculated from observation station data. The dataset 28 is available for download at https://doi.org/10.5683/SP3/4B18XZ, and derived visualization products can be 29 accessed across the web platform http://feux.escer.uqam.ca/.

Keywords. Canadian Forest Fire Weather Index (FWI) System, Wildfires, Severity Rating, solar noon, Canada.





1 Introduction

31

The Canadian Forest Fire Weather Index (FWI) System (Turner & Lawson, 1978; Van Wagner, 1985 & 1987; 32 33 Wang et al., 2015), which is part of the Canadian Forest Fire Danger Rating System (CFFDRS) developed by 34 Natural Resources Canada (NRCan), is used by many countries around the world (e.g., Australia, France, and 35 Portugal) for wildfire management, prevention and suppression . Notably, this digital system is widely utilized by 36 Canadian fire management agencies and international counterparts specifically to assess fire danger and potential 37 fire behavior of active wildfires. It is also widely used in the context of climate change (see Barnes et al., 2023) to 38 predict several fire regime variables (e.g., fire occurrence, annual area burned, fire season length). 39 The current FWI System, as defined in Van Wagner (1987), depends on readings taken each day at local 40 noon, either according to the time zone or standard UTC (Coordinated Universal Time), of the following surface 41 weather variables: the air temperature (at 2-m), the relative humidity (at 2-m), the wind speed (at 10-m) and the 42 accumulated precipitation during the previous 24 hours. Noon weather readings were chosen because the original 43 work on the FWI method demonstrated that these values can accurately predict fire danger at its mid-afternoon 44 peak at around 1700. However, this standard local noon method (referred to as the UTC method hereafter) has 45 several shortcomings for continuous and gradual calculation of indices across the entire Canadian territory. 46 Canada, spanning over 5,500 km from west to east, has six time zones across more than 95° of longitudes. 47 Calculating FWI at local noon within each time zone produces a significant temporal bias between the easternmost 48 and westernmost areas of the same time zone, since the same legal time is used regardless of the station's location 49 or where the meteorological data are collected. For example, Havre-Saint-Pierre (50° 14' N, 63° 36' W), in Eastern 50 Quebec, and Thunder Bay (48° 22' N, 89° 14' W), in Western Ontario (see Fig. A1, Appendix A), lie in the same 51 time zone, but are separated by almost 26° of longitude, leading to a time difference of about 104 minutes for the 52 sun to reach its zenith in each location. This can lead to substantial differences in the representativeness of the 53 most fire prone conditions during the day depending on the location, making it challenging to compare results both 54 between and within zones. Additionally, the elevation of the sun in the sky, and consequently the received solar 55 radiation influencing the local energy balance, can vary significantly at the same local time due to the longitudinal 56 extent of the time zone. 57 The other shortcoming of the UTC method is the discontinuity or heterogeneity of the calculated FWI fields 58 along the time zone boundary, especially when using gridded data (reanalysis or meteorological/climatological 59 model data) and even more so when the spatial resolution of reanalysis or gridded products increases. This is of

particular importance as fine- to medium-scale gridded daily weather data are becoming increasingly accessible





- 61 worldwide to calculate FWI components at regional and local scale (e.g., ERA5-Land reanalysis products; Munoz-
- 62 Sabater et al., 2021, high-resolution convection-permitting regional climate model). The abrupt change in legal
- 63 UTC time can lead to a sharp demarcation in the calculated FWI output fields. This discontinuity makes it
- 64 impossible or difficult to evaluate the various components included in the FWI System in the areas adjacent to two
- 65 different time zones.

2 Objectives

66

- 67 The main objective of this study was to create a fine-scale gridded dataset of the daily FWI System components
- 68 and other fire season related indices, that best reflects the physical reality, for monitoring, in retrospective (6-days
- 69 lag), the daily evolution of the fire danger across Canada.
- 70 In this paper, we describe the development and deployment of the ERA5-FWI-SN dataset, calculated
- 71 according to the local insolation conditions, i.e., the solar noon (SN) method, and using ERA5 reanalysis hourly
- 72 data (Hersbach et al., 2020). We also provide, in the results section, a comparison of the ERA5-FWI values
- 73 calculated using the new improved and more physically-based approach (SN method, ERA5-FWI-SN) with those
- 74 calculated following the local noon classical approach (UTC method, ERA5-FWI-UTC). Since the starting and
- 75 end dates of the FWI System calculations can have critical impacts on the resulting values, the analysis used to
- 76 identify the optimal approach for determining fire season onset (or start of the fire season) and the end of the fire
- 77 season across Canada, based on ERA5 data, is also provided. These are also used to calculate the length of the fire
- 78 season.

79 3 Data production and methods

80 3.1 Overview of the Canadian Forest Fire Weather Index (FWI) System calculation

- 81 The FWI System is composed of three fuel moisture codes, i.e., the Fine Fuel Moisture Code (FFMC), the Duff
- 82 Moisture Code (DMC) and the Drought Code (DC), as well as three fire behavior indices, i.e., the Initial Spread
- 83 Index (ISI), the Buildup Index (BUI) and the Fire Weather Index (FWI), calculated on a daily basis (Fig. 1). Their
- 84 calculation requires the following fire weather observations at local standard noon (following the standard UTC
- method, see Van Wagner and Pickett, 1985):
- Air temperature at 2-meters above ground (in °C);
- Relative humidity at 2-meters above ground (in %);
- Wind speed at 10-meters above ground (in km h⁻¹); and



96

97

98

99

100101

102

103104

105

106107

108

109



- Accumulated precipitation over the last 24 hours (in mm).
- It also requires the previous day's value of the following fuel moisture codes (start-up default value are used on the first day of the fire season):
- Previous day's FFMC (start-up default value is 85);
- 93 Previous day's DMC (start-up default value is 6); and
- Previous day's DC (start-up default value is 15).

Default start-up values for FFMC, DMC and DC represent their standard dryness state and provide a reasonable set of conditions for most spring conditions in Canada, northern United States, and Alaska (Lawson and Armitage, 2008; Canadian Forest Service, 1984). However, an overwinter adjustment of the DC is necessary if drought conditions from the previous fall are suspected at the beginning of the season (Hanes et al. 2020). More details about this overwintering adjustment are provided in section 3.3.3.

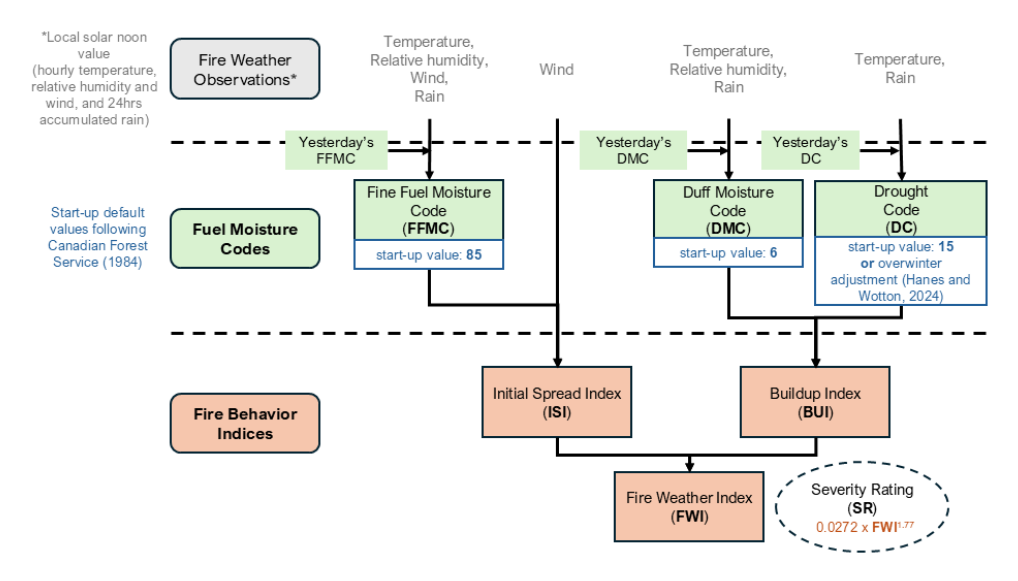


Figure 1: The Canadian Forest Fire Weather Index System and its input variables, modified from Lawson and Armitage (2008). Start-up default values are taken from Lawson and Armitage (2008) while the Severity Rating formula is taken from Van Wagner (1987).

3.2 Input dataset: hourly ERA5 reanalysis

As a first step, we used the hourly ERA5 reanalysis (Hersbach et al., 2020) with its original horizontal resolution of 0.25°, or about 31 km, for its near real time availability from 1950 to the present as a benchmark to develop the ERA5-FWI-SN gridded dataset across Canada. ERA5 reanalysis was provided by ECMWF (European Centre for Medium-Range Weather Forecasts) and accessed via the Climate Data Store (C3S, 2025) download platform. This fifth-generation reanalysis was developed by the ECMWF center via assimilation with the 4D-VAR method of





satellite observations and in situ meteorological data collected by the World Meteorological Organization (WMO; Hersbach et al., 2020). Access to the most recent ERA5 data, commonly referred to as ERA5T (see C3S, 2025), is limited to six days before the current day. Therefore, if the current day is July 10, the latest available data for

download dates to July 3, necessitating a six-days lag.

3.3 ERA5-FWI calculations and validation methods

3.3.1 The solar noon (SN) and local noon (UTC) methods

The SN method was developed to provide fire weather data based on a more "physical" approach. In contrast to the classical local noon time approach (UTC method), which results in arbitrarily assigned values based on common longitudes and not dependent on the seasonal cycle, the SN method is based entirely on the property of the sun's elevation above the local horizon, i.e., the local insolation conditions. The SN method also solves temporal biases and artifacts associated with the UTC method across time zones, thus allowing for a more homogeneous and spatially continuous field along time zone boundaries and across longitudes over Canada using medium—to fine—scale gridded data.

For both SN and UTC methods, we calculated the daily FWI System components across Canada, for each grid point of about 31 km spatial resolution of the ERA5 regular grid and for each day of the local fire season, from 1950 to 2024, following the more up-to-date guidelines from literature. For the four near-surface or surface meteorological controls of fire weather, i.e., hourly temperature, relative humidity, wind speed, and 24-hour accumulated precipitation, we selected (or in the case of precipitation, calculated) values either at local solar noon (SN method) or at local noon (UTC method). These values were then used to calculate the six standard daily components of the FWI System. Daily maximum temperature (tasmax) and daily mean snow depth (sdmean) were also calculated from hourly fields to determine, each year, the beginning (onset) and the end of the fire season (see the upcoming Section 3.3.2 for calculation methods). Daily sdmean was aggregated from hourly snow depth (sd, in meters), which was calculated following Eq. (1) from hourly ERA5 snow water equivalent (swe, in meters) and snow density (rsn, in kilogram per cubic meter) variables:

$$sd = \frac{swe \times \rho_{water}}{rsn} \tag{1}$$

where ρ_{water} represents the water density, estimated at 1,000 kg m⁻³.

To calculate the FWI System components using the UTC method, we used a time zone mask that allowed us to identify the correct time zone for each grid point (i.e. pair of latitude and longitude coordinates), and therefore





the respective UTC time, corresponding to the local noon time. Input weather parameters were then selected at the corresponding UTC time for FWI calculation.

To calculate the FWI System components using the SN method, we selected the input weather parameters at the time corresponding to when the sun reaches the local meridian (i.e., the highest position of the sun in the sky) for each grid point and for each day. Local solar noon at each location on Earth's surface was determined following Duffie et al. (2020). A longitude correction was first applied to the local time (1° of longitude corresponds to a time difference of 4 minutes). A correction called the "equation of time" was then applied, which corresponds to the fact that the Earth does not always move at the same speed on its orbit, so the sun can appear at the zenith with a deviation of up to ± 16 minutes compared to the local time or UTC.

The final correction equation for solar noon is therefore:

$$SNT = LT + LC + ETC$$
 (2)

where *SNT* corresponds to the solar noon time, *LT* the local time, *LC* the longitude correction, and *ETC* the equation of time correction.

The calculation of solar noon was performed using the Python library "daylight" (Python Package Index - PyPI, 2020) which allows the obtention of the solar noon time in UTC from geographic coordinates. Since the meteorological variables from the ERA5 reanalysis are provided on an hourly basis Coordinated Universal Time (UTC), the local solar noon corresponding value for each variable was calculated using a temporal proximity proportion or weighted average value that was applied between the two temporally closest fields. For example, if for a grid point the solar noon of the day was calculated at 18:20 UTC, the field value had to be weight-averaged using the 18:00 UTC and 19:00 UTC fields using 2/3 and 1/3 as the respective weights. This technique allows for a spatially explicit calculation of the various indices that eliminate artifacts along time zone boundaries across Canada.

For both methods, we used a Python code composed of six functions that we derived from the *fwi* function of the Canadian Forest Fire Danger Rating System (*cffdrs*) R library (Wang et al., 2024). This library was developed to calculate fire danger indices for single meteorological stations and was therefore adapted for model data or gridded data in NetCDF format, in Python programming language. In addition to the six FWI System outputs, we calculated the Daily Severity Rating (DSR), which is a numerical assessment of the difficulty or effort expected to control fires, as well as the cumulative DSR over each fire season (DSRc), which gives a relevant indication of fire severity over an entire season. DSR was calculated following Eq. (3):

$$DSR = 0.0272 \times FWI^{1.77} \tag{3}$$





3.3.2 Fire season onset and stop

By convention, the FWI System calculations are stopped at the end of the fire season and are restarted the next spring, on onset day, using the start-up default values for FFMC, DMC and DC components. We defined the end of the fire season (WinterOnset) following the approach outlined by Wotton and Flannigan (1993), as the fourth day following three consecutive days with daily maximum temperature (*tasmax*) < 5°C. For fire season onset calculation, we considered not only temperature conditions, but snow conditions as well, since the snow cover, in snow-covered regions, plays a major role in the determination of the fire season onset. Also, the snow cover's important variability across the country makes it essential to distinguish between areas where the fire season onset depends on its ablation, and those where the onset depends solely on temperature conditions. Also, important changes in the snow cover that occurred since 1950 and that will continue in the future have already impacted the fire season onset, leading to earlier onset dates (Jain et al. 2017). In snow-covered regions, the initiation of the calculation in the spring is scheduled to start the first day of the year following three consecutive days with no snow cover and with *tasmax* greater than 12°C while it is scheduled to occur the first day of the year following three consecutive days with *tasmax* greater than 12°C for non-snow-covered regions, according to Turner and Lawson (1978). Snow-covered regions are defined as regions where at least 75% of the days in January and February have a mean snow depth value of 0.10 m or greater (CWFIS, n.d.).

However, considering the snow condition in snow-covered regions for onset calculation across Canada and using gridded data is a challenge, due to the poor quality of gridded data snow products. We found that using ERA5 reanalysis data was leading to important delays in ablation of snowpack in the spring, that did not correspond to the ablation date given by satellite observation data, especially in the Rocky Mountains or surrounding areas (see Appendix A, Fig. A1), which was also mentioned in other studies (Kouki et al., 2023; Lei et al., 2023; Hersbach et al., 2020). Moreover, during data preparation and exploration phase, we found that some grid points in mountainous areas (Rocky Mountains for example) would never show 3 consecutive days with a snow depth value of 0 meter for some years, which was again inconsistent with satellite-based observations. We found that using a snow depth threshold value of 0.01 meters instead of 0 meter, in the application of the snow condition, would lead in a more accurate onset date.

We therefore adapted the methodology for calculating onset using ERA5 data, utilizing temperature and snow conditions, with a snow depth threshold set at 0.01 meters ("TS" method). Snow conditions were verified using the daily mean snow depth (*sdmean*) and no onset was calculated for regions where *sdmean* never reaches values below 0.01 meters. Appendix B provides a comparison between onset values calculated using the "TS" method,



199

200

201

202

203

204

205

206

207

208

209

210

211

212

213

214

215

216

217

218

219

220

221

225



and onset values calculated using only temperature conditions ("T" method) or using temperature and snow conditions with total snow ablation ("TS0" method).

3.3.3 Overwintering adjustment of the DC

In Canada, it is assumed that FFMC and DMC reach the moisture saturation point of winter precipitation at the time of spring melt. This assumption is reasonable because the assumed initial conditions disappear rapidly after a few days. However, due to the relatively long response time of the DC fuel layer (around 53 days under normal conditions), any bias in the estimation of this starting condition before the arrival of spring or thawing conditions can affect the DC at the beginning of the fire season (Hanes et al. 2020). If the fuel layer required for the DC calculation does not fully reach saturation when the snow melts in the spring, an overwintering adjustment of the DC start-up value needs to be applied, which is often the case in the dry areas of the Canadian Prairies (de Groot et al., 2015). At each year's start-up date, we applied the overwintering procedure of the DC for the regions where the last DC value from the previous fire season (DCf) was far from saturation, i.e., ≥ 50, following Hanes and Wotton (2024), and used start-up default value of 15 elsewhere. This recent study shows that this criterion (DCf≥ 50) is a better indicator of abnormal dry conditions during the previous fall and winter than the accumulated precipitation during winter (rw) threshold of $rw \le 200$ mm, proposed by Lawson and Armitage (2008). DCf and rw normal values maps can be found in Appendix C. Their values reveal that the overwintering adjustment of the DC applies in more areas when using the DCf criteria (Appendix C, Fig. C1) than when using the accumulated precipitation during winter (Appendix C, Fig. C2). However, using DCf criteria instead of rw will affect DC startup values only for few grid cells outside of the area where $rw \le 200$ mm, with a calculated DC start-up value of 15 in most cases (Appendix C, Fig. C3). Nevertheless, using the DCf criteria still leads, most of the time, into more areas with higher DC start-up values in west and central parts of Canada, with persistent effects on the following seasons, as revealed for years 2022, 2023 and 2024 (Appendix C, Fig. C3). The equations for the DC overwintering adjustment, given by Turner and Lawson (1978), are as follows:

• DC moisture equivalent at the end of fall (Qf):

222
$$Qf = 800 \times exp\left(\frac{-DCf}{400}\right)$$
 (4)

• DC moisture equivalent at the beginning of spring (Qs):

$$224 Qs = a \times Qf + b \times (3.94 \times rw) (5)$$

• DC obtained for the beginning of the fire season (DCs):





 $DCs = 400 \times log \left(\frac{800}{Qs}\right) \tag{6}$

where *DCf* corresponds to the DC value at the end of the previous fire season, *a* corresponds to the carry-over fraction of last fall's moisture, *b* corresponds to the wetting efficiency fraction, which corresponds to the effectiveness of winter precipitation in recharging depleted soil moisture reserves in the spring, and *rw* corresponds to winter precipitation (in mm).

The accumulated precipitation during winter (rw) was calculated, locally, from the day following the end of the previous fire season to the next fire season (i.e., to define the onset value). We used a value of 1.0 for the carry-over fraction (a) and a value of 0.5 for the wetting efficiency fraction (b), as suggested by Hanes and Wotton (2024).

3.4 Data validation

The ERA5-FWI-SN and ERA5-FWI-UTC daily FWI values were validated with the CWFIS-FWI, which corresponds to the FWI calculated from observation station data at local noon by the CWFIS across their network in Canada (see their locations in Fig. D1, Appendix D). Data was validated between 2015 and 2024 (years of available observed data) and the comparison was made by selecting the closest grid point (ERA5-FWI-SN and ERA5-FWI-UTC) to each station (CWFIS-FWI). Independent FWI calculation from CWFIS observation station data using both UTC and SN methods was not feasible, as the organization only supplied the daily FWI values.

3.5 ERA5-FWI-SN dataset and automation

Finally, the gridded daily FWI System components (FFMC, DMC, DC, ISI, BUI and FWI) calculated across Canada using the SN method, including the DSR index, were formatted into standard NetCDF and GeoTIFF files for sharing via the ERA5-FWI-SN dataset and for further analysis. Other indices related to the fire season (the start of the fire season, i.e., Onset, the fire season end, i.e. WinterOnset, the length of the fire season, i.e., FSL, and the cumulative Daily Severity Rating, i.e., DSRc) were also added to the dataset. Table 1 provides an overview of the indices available in the ERA5-FWI-SN dataset. The dataset covers the land masses of Canada at a spatial resolution of about 31 km from 1950 up to now (6-days lag). The calculations were initialized in 1950 using DC, DMC and FFMC start-up default values. For the subsequent years, we followed the overwintering procedures to adjust, if necessary, the DC start-up value.

Table 1: Description of the daily FWI components and related yearly indices included in the ERA5-FWI-SN dataset, available for download in NetCDF or GeoTIFF format at https://doi.org/10.5683/SP3/SA1WEL (Benoit et al., 2025)



256

257

258

259

260

261

262

263

264

265



Component or Index	Long name	Units							
Daily components									
FWI	Fire Weather Index	1							
BUI	Buildup Index	1							
DC	Drought Code	1							
DMC	Duff Moisture Code	1							
FFMC	Fine Fuel Moisture Code	1							
ISI	Initial Spread Index	1							
DSR	Daily Severity Rating	1							
	Yearly indices								
DSRc	cumulative Daily Severity Rating	1							
Onset	Fire Season Onset	Julian day							
WinterOnset	Fire Season End	Julian day							
FSL	Fire Season Length	day							

An automation process, carried out at the ESCER Centre, was also set up in order to calculate the FWI System components every day with a 6-days lag, corresponding to the latest ERA5 available data for download, and to update the dataset daily. The automation process has an execution time of approximately 1 hour, depending on the speed of access (download time) to ERA5 reanalysis data and ensure that the following steps are carried out every day of the year at 02:00 AM (i.e., 07:00 UTC), namely:

- The download of the latest available fire weather input data (with a 6-day lag from the current time, i.e., j-6) from the "ERA5 hourly data on single levels from 1940 to present" dataset via the Copernicus CDS Application Program Interface (API) download service (see C3S, 2025).
- 2) The formatting of all fire weather input data from ERA5 to enable the calculation of the FWI System components, including the calculation of hourly wind speed, relative humidity and snow depth.
- 3) The calculation of the fire season onset (Onset), the start of the overwintering period (WinterOnset), the accumulated precipitation during winter (WinterRain) and the fire season length (FSL).
- The calculation of the daily FWI System components (including the DSR and DSRc indices) using the
 SN method.





- 5) The download of the latest FWI values calculated by the CWFIS (CWFIS-FWI) from observation station data (https://cwfis.cfs.nrcan.gc.ca/downloads/fwi_obs/current/), i.e., nearly 650 meteorological stations on average, depending on the day (the location of the CWFIS stations network is provided in Fig. D1 in Appendix D).
- 6) The calculation of statistics and correlations between CWFIS-FWI and ERA5-FWI-SN daily FWI values for all available stations and their corresponding grid point, including the preparation of the daily map showing these values and correlations.
 - 7) The production of daily maps for FWI comparison with historic daily records, recalculated yearly, at the end of the year, to include all data since 1950.
- 8) The preparation of the daily GeoTIFF files for all the FWI System components for interactive viewing on the website (http://feux.escer.uqam.ca/en/viewer.html).
 - The standardization of updated daily FWI components files in NetCDF and GeoTIFF formats for their storage in the ERA5-FWI-SN dataset.

4 Results

4.1 Fire-weather index climatology

We produced the climatology of the monthly mean FWI, calculated between 1950 and 2024, for the months of June, July, and August, for both SN (Fig. 2a) and UTC (Fig. 2b) methods. In both cases, most of the highest FWI values are located south of Alberta and Saskatchewan with normal values reaching up to, respectively for SN method and UTC method, 18 and 17 in June, 26 and 25 in July, and 29 and 28 in August. This area of highest FWI values, largely covered by agricultural prairies, does not have forests prone to large vegetation fires. However, annual dry weather conditions combined with high temperatures in summer generate high FWI values. The area located around the Great Slave Lake in the Northwest Territories (see Fig. A1, Appendix A) also exhibits high FWI in June, with monthly mean values reaching up to 18 for SN method and 17 for UTC method. The south of British Columbia is the second area with the highest FWI normal values for the months of June and July, with values exceeding 15. Overall, the average monthly mean FWI values for the Canadian provinces and territories are between 2 and 10 either for June, July or August, with an average value around 5 for the entire country.



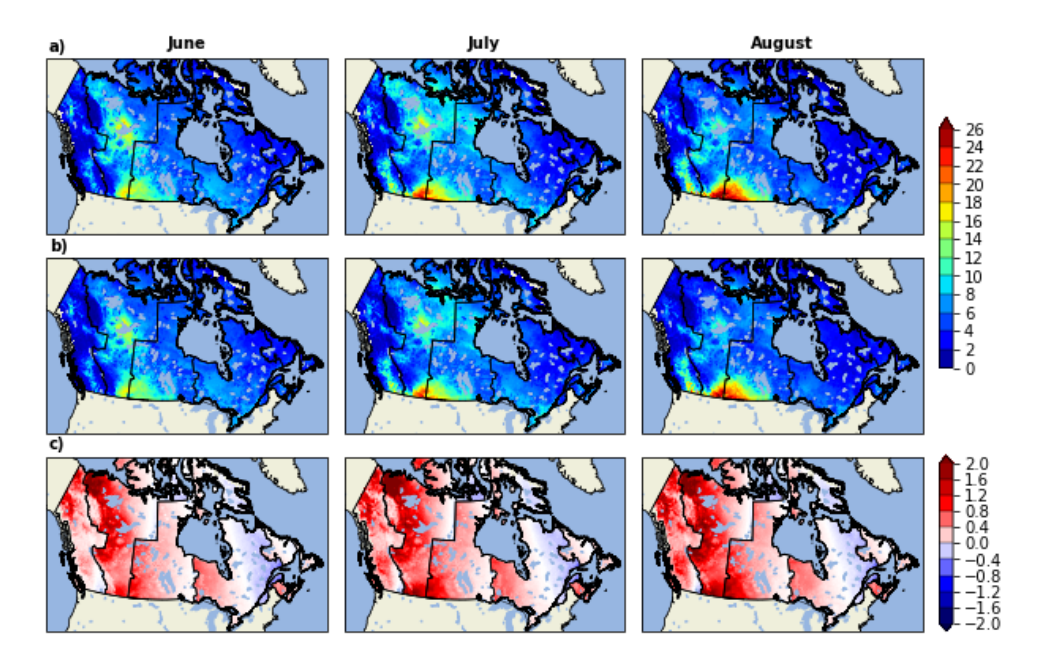


Figure 2: Climatology between 1950 and 2024 of the monthly (June, July, and August, left to right panels, respectively) mean FWI values obtained with a) the solar noon (SN) method, and b) the local noon (UTC) method. The differences in the monthly (June, July, and August) mean values between these two fields (i.e., a - b) are shown in panels c). FWI were all calculated using the ERA5 reanalysis hourly data.

4.2 Comparison of the solar noon (SN) and the local noon (UTC) methods

The SN method aims to diminish the abrupt change in component values between two provinces with different time zones both over the western and eastern areas due to the change in local time. The differences between the two methods (SN minus UTC methods) for June, July and August FWI monthly mean value (Fig. 2c), reveal higher values over western time zones from SN method than UTC ones, and discontinuities between time zones (up to +3.4 in July west of Alberta, west of the daylight time and up to +2.6 in August west of Saskatchewan). Over the longest time zone located in eastern Canada covering Québec and Ontario (i.e., eastern daylight time -EDT, extending approximately 1,900 km from East to West with a temporal lag of 68 minutes in local time calculation), slight negative values (around -0.6) are present in the east and moderate positive ones (>1) using the SN method with respect to the UTC method. The higher positive differences of FWI monthly mean values are located over western time zones, in central and mountain daylight time zones (see Fig. 2c).

As for the FWI index (see Fig. 2), the UTC method tends to generate higher/lower DSRc values in the eastern/western part of the EDT time zone than the SN method (Fig. 3b). These higher DSRc values are also particularly pronounced over central and mountain daylight time zones, with strong discontinuities between two consecutive time zones (Fig. 3a). For these cumulative DSR, as defined in Eq. (3), the differences increase between



the two (SN and UTC) methods over the whole fire season, as changes in the local time vary during the year and not only during the day.

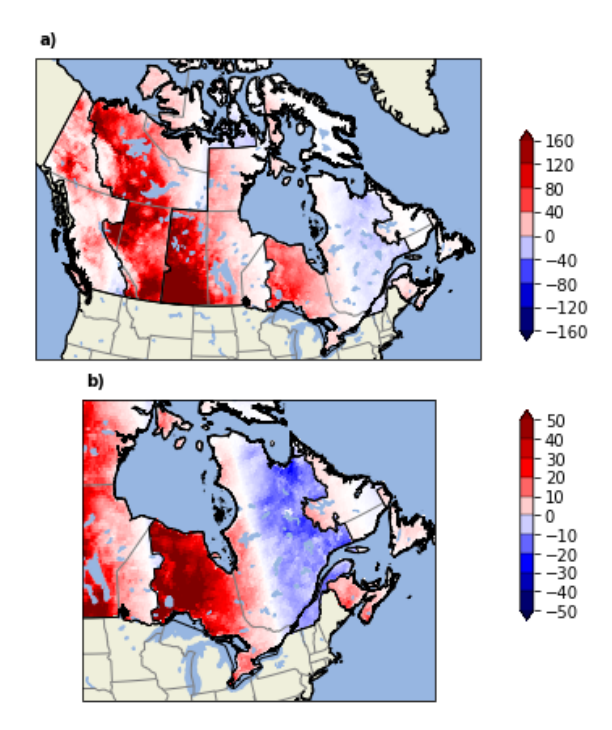


Figure 3: Differences between solar noon (SN) and UTC methods for the ERA5 cumulative Severity Rating (DSRc) index for the year 2023 for a) Canada and b) eastern Canada with a readjusted scale. The black isolines correspond to the delimitation of time zones.

4.3 Fire season onset climatology and trends

Using ERA5 reanalysis data and the method that considers both snow and temperature thresholds in snow-covered regions, and temperature threshold in non-snow-covered regions, to calculate fire season onset (i.e. see method "TS" in Appendix B), we found that onset happens first in south west Prairies and in the southernmost area of Canada, northside of Lake Erie (between March 15th and April 1st), as shown by the onset normal values map for 1991-2020 period on Fig. 4. On average, in the Boreal Forest and Woodland of Canada, fire season normally starts between May 6th and June 8th, with the earlier onset happening in the West-Central Boreal Forest, as early as April 9th, and the latest in the Atlantic Maritime Heathland (onset ranging between May 8th and July 21st) and in the Subarctic Woodland-Tundra (onset ranging between May 22th and July 24th). Without considering the Arctic Tundra, where fires are scarce, the latest onset dates are found over the Rocky Mountains and other mountainous areas of Canada (between June 15th and July 1st, on average) due to the persistence of snow until early summer.



Between 1950 and 2024, changes in temperature and snow conditions during spring led to earlier onset dates in most of the forest dominated areas of Canada. While the diminution of snowpack in westernmost regions of Canada greatly contributed to earlier onset in that area, more than temperature warming did alone, as shown by calculated trends in Figs B2, B3 and B4 of Appendix B.

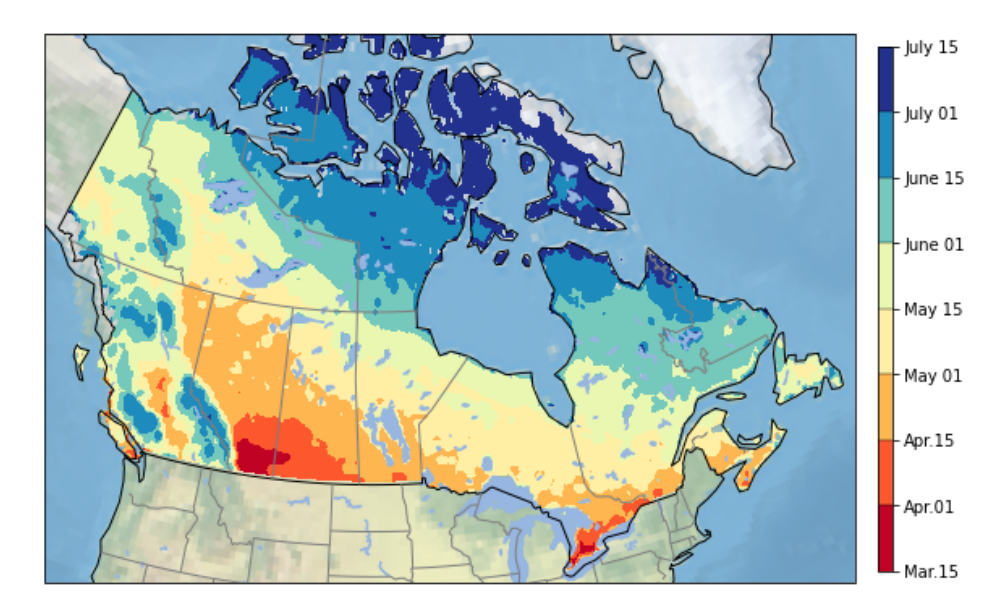


Figure 4: Fire season onset climatology (1991-2020). Onset normal values were calculated using the TS method, which considers temperature and snow conditions in snow-covered regions, using a snow depth threshold value of 1 cm.

4.4 ERA5-FWI validation with CWFIS-FWI

Table D1 in Appendix D presents Pearson (temporal) correlation coefficients calculated on a daily scale for each month from May to September and for each year from 2015 to 2024 between the CWFIS observed FWI, and those calculated using the ERA5 reanalysis for both SN and UTC methods. The average correlation with meteorological stations varies from 0.70 to 0.86 depending on the month and the year, with very similar results between the two methods.

The Taylor diagram statistics (Fig. 5) reveal that both methods produce FWI values that are very well spatially correlated with observations for most of the stations (median of 0.81 for both methods), with very similar results between the two methods. The normalized standard deviation for both methods (median of +1.09 for UTC method and +1.06 for SN method) indicates a slight overestimation of the spatiotemporal variability with respect to observations, with a slightly lower bias obtained with the SN method (Fig. 5). The RMSEs are also similar between the two methods, with relatively low values on average (median value slightly over 0.6 in both cases, Fig. 5).



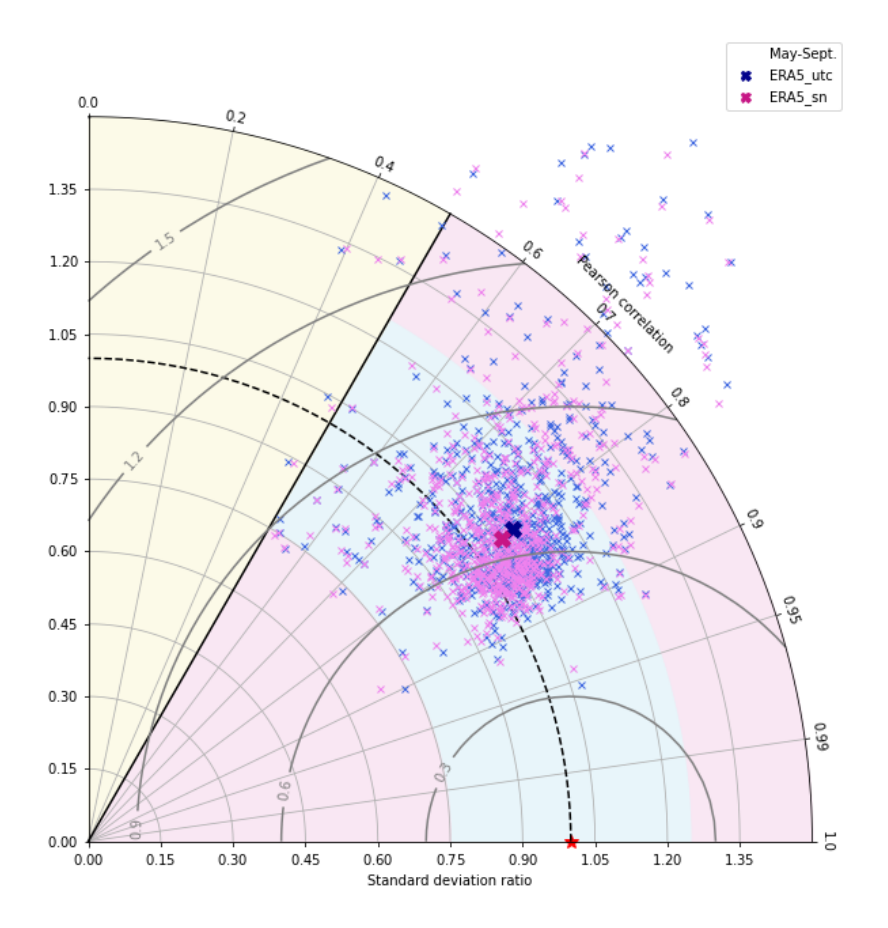


Figure 5: Taylor diagrams statistics (standard deviation, Pearson correlation, and RMSE—Root Mean Square Error) between the ERA5 FWI calculated using the UTC method (ERA5_utc in blue) and using the SN method (ERA5_sn in violet) and the Canadian Wildland Fire Information System (CWFIS) FWI calculated from observation station data. Statistics were calculated between the daily FWI values and are summarized from May 1st to September 30th for years 2015 to 2024 for all available stations. All values were normalized with respect to the observations (CWFIS FWI), represented by the red star. The curved lines correspond to the normalized RMSE, and the big dark blue/violet cross to the median values of the UTC/SN method statistics from all pairs of grid points and observation stations data (small cross).

5 Data availability

The full time series (1950 to the most recent full year available) of the daily FWI System components and other fire-season-related indices (Table 1) is available as the ERA5-FWI-SN dataset in both NetCDF and GeoTIFF formats via the Borealis platform at https://doi.org/10.5683/SP3/4B18XZ (Benoit et al., 2025), as the ERA5 dataset. A direct link to the dataset is also provided in the "Data Access" section of the project website:



http://feux.escer.uqam.ca/en/data_access.html. A Web Map Service (WMS), currently under development, will also allow users to access the mapped data directly through geospatial applications or software.

Both static and interactive visualizations of the daily FWI components and related analyses are available on the website. The homepage (http://feux.escer.uqam.ca/en/index.html) features a static map of the most recent FWI values across Canada, along with two additional maps comparing current FWI values to historical records (see Fig. 6 for example and refers to step 7 in section 3.5). A more detailed map of daily FWI values, including a comparison with CWFIS-FWI values (see Fig. 7 for example and refer to step 6 in section 3.5), is also available for download in PNG format for any day since 2021 in the "FWI" section (http://feux.escer.uqam.ca/en/fwi.html). Finally, interactive viewing of daily FWI components values since 2021 is available in the "Data Viewer" section (http://feux.escer.uqam.ca/en/viewer.html).

FWI breaking records (2025/05/29)

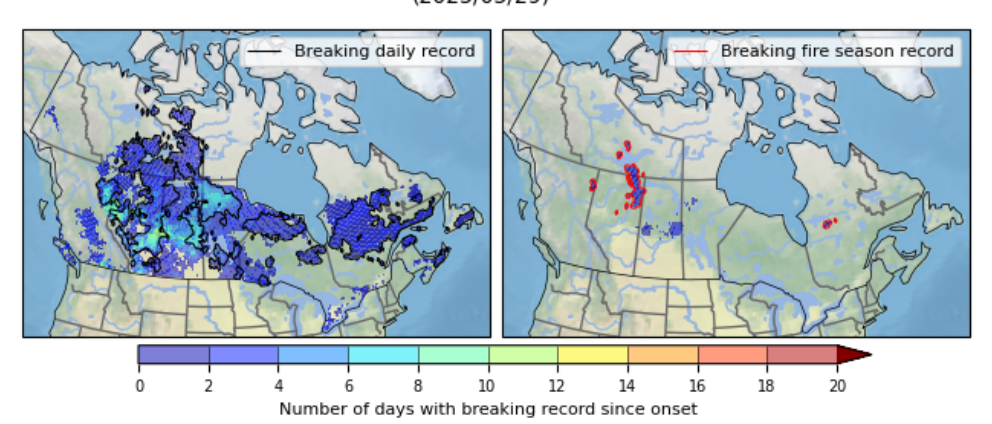


Figure 6: FWI breaking records for May 29th of 2025 across Canada. The left panel map shows areas with FWI values breaking the daily record (for May 29th, in black contours) while the right panel map shows areas with FWI values breaking fire season record (considering the entire fire season, in red contours) for the current day. Colormap represents, locally (spatial resolution of approximately 31 km), the number of days where the daily FWI has been breaking records since the onset. Historical records were calculated over the period 1950-2024.



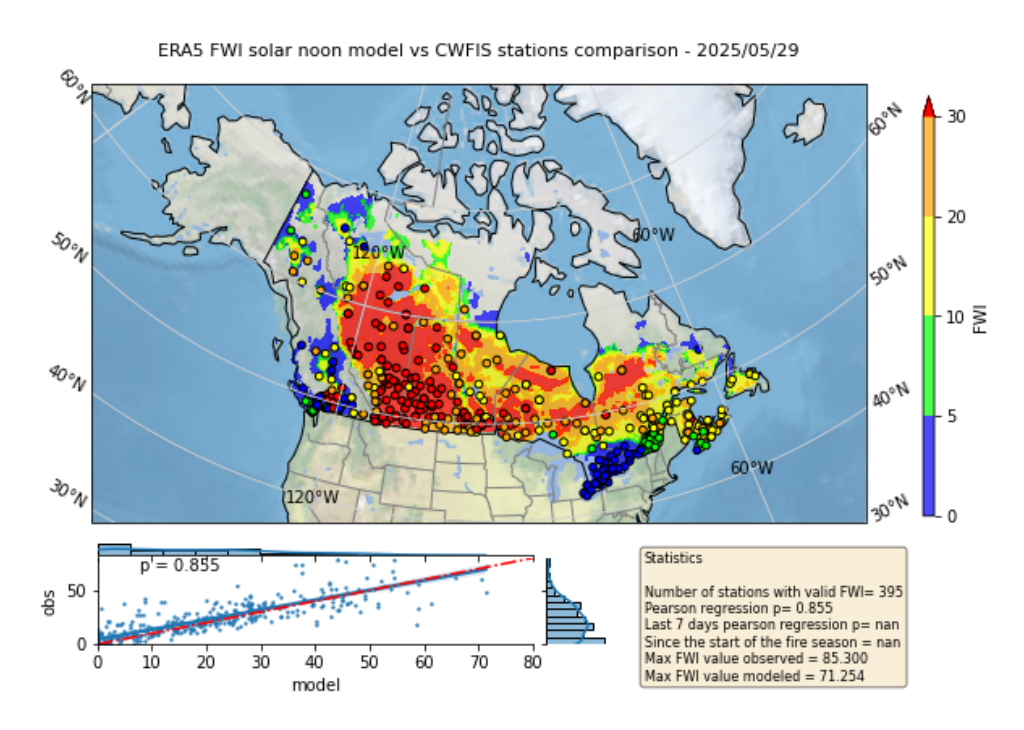


Figure 7: FWI daily value for May 29th of 2025 across Canada, at a spatial resolution of approximately 31 km, calculated using ERA5 reanalysis data (colormap) and its comparison with FWI values calculated from CWFIS observation station data (point markers). This daily map can be found in the website "FWI" section at http://feux.escer.uqam.ca/en/fwi.html.

6 Code availability

380 381

382

383

384

385

386

387

388

389

390

391

392393

394

395

396

The codes used to generate the dataset and visualization products (steps listed in the automation procedure in section 3.5), are available at https://github.com/risqueescer/fwi_docker and consist in the following three main types of codes:

- Python scripts to download ERA5 data via queries to the public CDSAPI servers (C3S, 2025) and generate the dataset.
- Python scripts to download CWFIS data and perform comparative analysis between ERA5-FWI and CWFIS-FWI.
- 3) Python scripts to produce analysis and visualization products for the FWI components.

7 Discussion and further works

The new solar noon (SN) method applied to calculate the daily FWI System components using ERA5 hourly reanalysis data provides more consistent and plausible values across Canada, especially along the western parts of





the daylight time zones, and prevent discontinuities in component values over these areas. The FWI values from this new method are also compatible with the ones calculated from the CWFIS meteorological weather stations network. Our dataset also offers significant improvements over the FWI dataset based on the ERA5 reanalysis developed by ECMWF (Vitolo et al., 2020), which relies on the UTC method for its calculations. Additionally, these FWI calculations omit both the start and end-of-fire-season rules, as well as any overwintering procedures at the onset of the season. In fact, we have clearly demonstrated the importance and advantage of both considering the overwintering procedures to potentially adjust the DC start-up value, and the local solar noon approach, in providing more physical gridded values of FWI components over different climatic conditions across Canada.

The new ERA5-FWI-SN dataset and related products were made available at the ESCER website: http://feux.escer.uqam.ca. However, as noted in the recent study over Sweden in Sjöström et al. (2025), moderate to high ERA5-based FWI were underestimated with respect to the values based on observations. In our case, we can see from Fig. 6 that maximum FWI values > 85 are observed from CWFIS station data (on May 29th, 2025) whereas ERA5-FWI-SN maximum values are only around 71. This implies that checking extreme-value biases against point observations need to be made in future studies. In fact, to document these potential biases, we verified all daily values of FWI during the fire season across Canada, between CWFIS stations and ERA5 reanalysis, since 2015 at intra-annual and interannual scales.

In the near future, we plan to use the SN method to identify and evaluate the changes in the FWI System components and in forest fire danger from high resolution regional climate model simulations under climate change. This will be done with simulations from the latest version of the new Canadian regional climate model (CRCM version 6, i.e. CRCM6 used and described in Llerena et al., 2023, and Roberge et al., 2024), developed at the ESCER center, in middle/long-terms or climate mode (i.e. under seamless prediction) from the available analyses and simulation ensembles of the GEPS/GDPS (Global Ensemble Prediction System/Global Deterministic Prediction System) and/or RDPS (Regional Deterministic Prediction System) of Environment and Climate Change Canada, and CMIP6 climate simulations (see Intergovernmental Panel on Climate Change (IPCC), 2021). The CRCM6 configuration with a 12 km horizontal resolution and covering all North America will be used for this purpose. Preliminary results revealed the feasibility of this approach, since the 6- or 3-hourly variables are available to drive the CRCM6 at the lateral boundaries (i.e., simulated climate variables from Global Climate Models used to downscale climate information at the regional scale from Regional Climate Model, see further details in Chapter 10 of the last IPCC report; Doblas-Reyes, 2021).

https://doi.org/10.5194/essd-2025-535

Preprint. Discussion started: 19 November 2025

© Author(s) 2025. CC BY 4.0 License.





Further works also need to be done to assess the changes in forest fire danger at the ecosystem scales from the convection-permitting configuration of the CRCM6 model (at resolution < 4 km, see Benoit et al., 2022; Llerena et al., 2023; Roberge et al., 2024) to evaluate how the mesoscale convection systems, that affect ignition of vegetation fires from thunderstorms and their associated lighting occurrences, will be modified under climate change. The SN method will then be relevant for such purposes, to prevent discontinuities across the longitudes of single point indices value (revealed in the UTC method), more pronounced at higher resolution. This will also improve our collective capacity to better anticipate and consider higher temporal and spatial weather conditions that could trigger severe and extensive forest fires across Canada, as those experienced during the fire season of 2023 (see Boulanger et al., 2025; Barnes et al., 2023).

The website http://feux.escer.uqam.ca is under constant development and improvement and should soon propose the same FWI-SN products as generated using the ERA5 reanalysis data for the historical period, but using the CRCM6 simulation data. Products related to changes between future and historical FWI should also be available soon after CRCM6 future simulations will be completed. More interactive plots to allow FWI analysis at different time and space levels will also be deployed. Finally, any changes that would be made to the FWI dataset will be announced on the website and detailed in the "Methods" section (http://feux.escer.uqam.ca/en/methodology.html).

https://doi.org/10.5194/essd-2025-535 Preprint. Discussion started: 19 November 2025 © Author(s) 2025. CC BY 4.0 License.

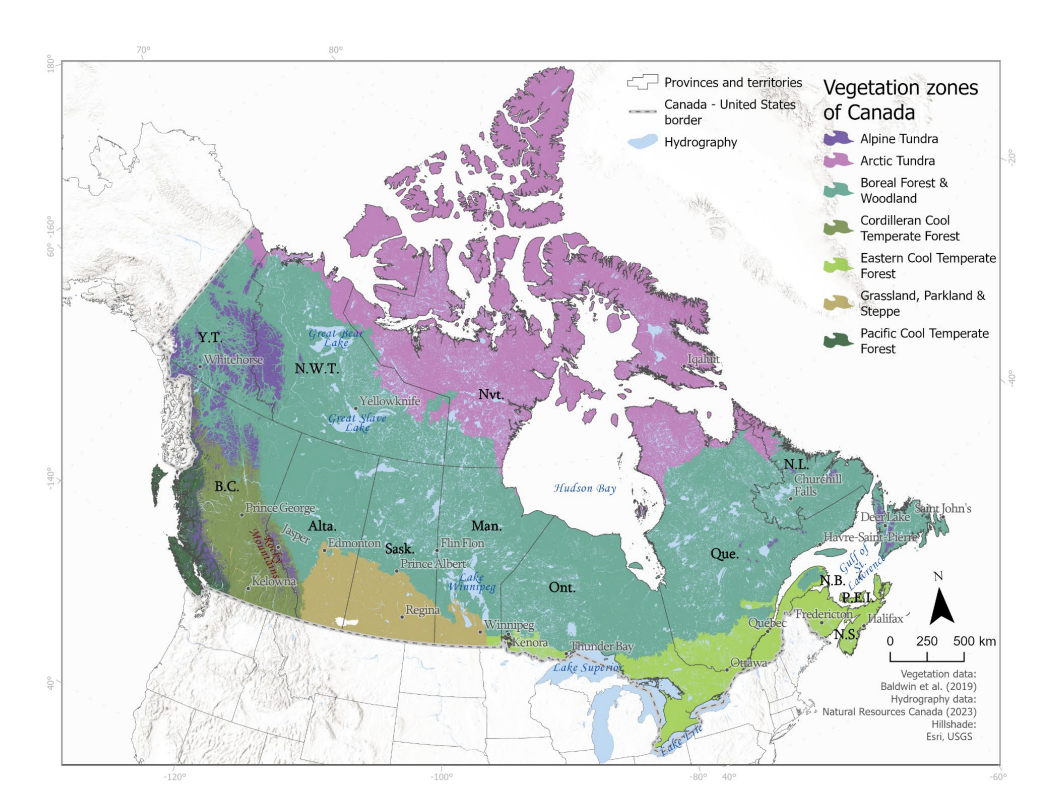




442 Appendices



443 Appendix A – Study domain map



444445

446

Figure A1: Study domain, i.e., land masses of Canada, including the delineation of the provinces and territories, and of the vegetation zones of Canada (Baldwin et al., 2019). The map shows important places with their toponym, mentioned or not in the paper, for a better overall comprehension.



452453

454

455

456

457

460461

462

463

464

465466

467

468 469

470



Appendix B - Onset calculation methodology and analysis

- Each year, for grid points that report significant snow cover during the winter (i.e., ≥10 cm, this snow cover threshold occurrence represents at least 75% of the days in January and February), we calculated the onset date using the three following methods:
 - "TS" method: Onset occurs on the day following 3 consecutive days with snow depth lower than 1 cm and maximum daily temperature higher than 12°C;
 - "T" method: Onset occurs on the day following 3 consecutive days with maximum daily temperature higher than 12°C;
 - 3) "TS0" method: Onset occurs on the fourth day following snow ablation (snow depth of 0 cm). For the previous 3 days, snow depth value needs to be of 0 cm and maximum daily temperature higher than 12°C.
- For grid points that don't report significant snow cover during the winter, onset was calculated following the temperature condition ("T" method) only.

The onset climatology (1991-2020) for the "TS" method is shown in Fig. B.1a as well as its difference with the onset climatology calculated using the "T" method (Fig. B1b, "T" - "TS") and the "TS0" method (Fig. B1c, "TS0" - "TS"). The latest onset values calculated over the Great Bear Lake and the Great Slave Lake (between June 8th and August 9th, Fig. B1a) are in adequation with climate observations found in the literature which say that the Great Bear Lake is covered with ice from late November to July (Hebert, 2007), with daily mean temperature normal values exceeding 12°C only in July (Environment and Climate change Canada). When considering only the temperature condition ("T" method), onset happens earlier in snow-covered regions (2 days earlier on average but can be up to 54 days earlier in mountainous regions) than when considering both temperature and snow condition with a threshold value of 1 cm ("TS" method) (Fig. B1b). When considering the complete snow ablation with ERA5 reanalysis data ("TS0" method), onset occurs later than the ones from "TS" method (5 days later on average, but up to 26 days later in some areas) (Fig. B1c).

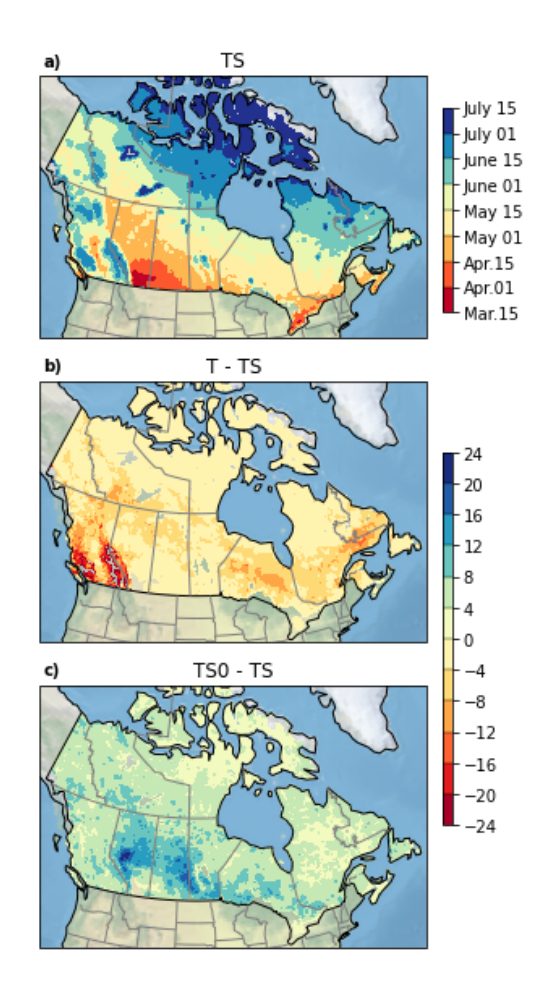


Figure B1: Fire season onset climatology (1991-2020) and its comparison with onset calculated using different methods. In a) onset normal values are shown and were calculated using the "TS" method, which considers temperature and snow conditions in snow-covered regions, using a snow depth threshold value of 1 cm. In (b) difference between onset normal values, calculated using the "T" method, which only considers temperature conditions in snow-covered regions, and "TS" onset normal values. In (c) difference between onset normal values, calculated using the "TS0" method, which considers temperature and snow conditions in snow-covered regions, using a snow depth threshold value of 1 cm, and "TS" onset normal values. Values in panels (b) and (c) correspond to the onset date difference given in number of days.

Trends calculated on the fire season onset date, over the whole time window between 1950 and 2024, show that the snow and temperature conditions changed leading to an earlier season start-up, a trend significant (p-value < 0.05) for the whole study area, including most of the forest dominated areas of Canada, for both "TS" and "T" methods (Figs. B2 for onset days and B3/B4 for snow/temperatures trends). However, changes in snow conditions contributed to more significant grid points with changes in fire season onset time, and more important changes in values, with onset occurring up to more than 30 days earlier in British Columbia (Figs. B2a and B2c). Figures B3 and B4 show the trends in snow depth values on February, March, April and May 15th and the monthly mean value of the maximum daily temperature for the same months, calculated over the period from 1950 to 2024. Both





- variables reveal their influence on the onset date trend with an important decrease in snow depth values in British
- Columbia (Fig. B3), and important increases in temperature over a major part of the Boreal Forest, especially in
- 489 May (Fig. B4).

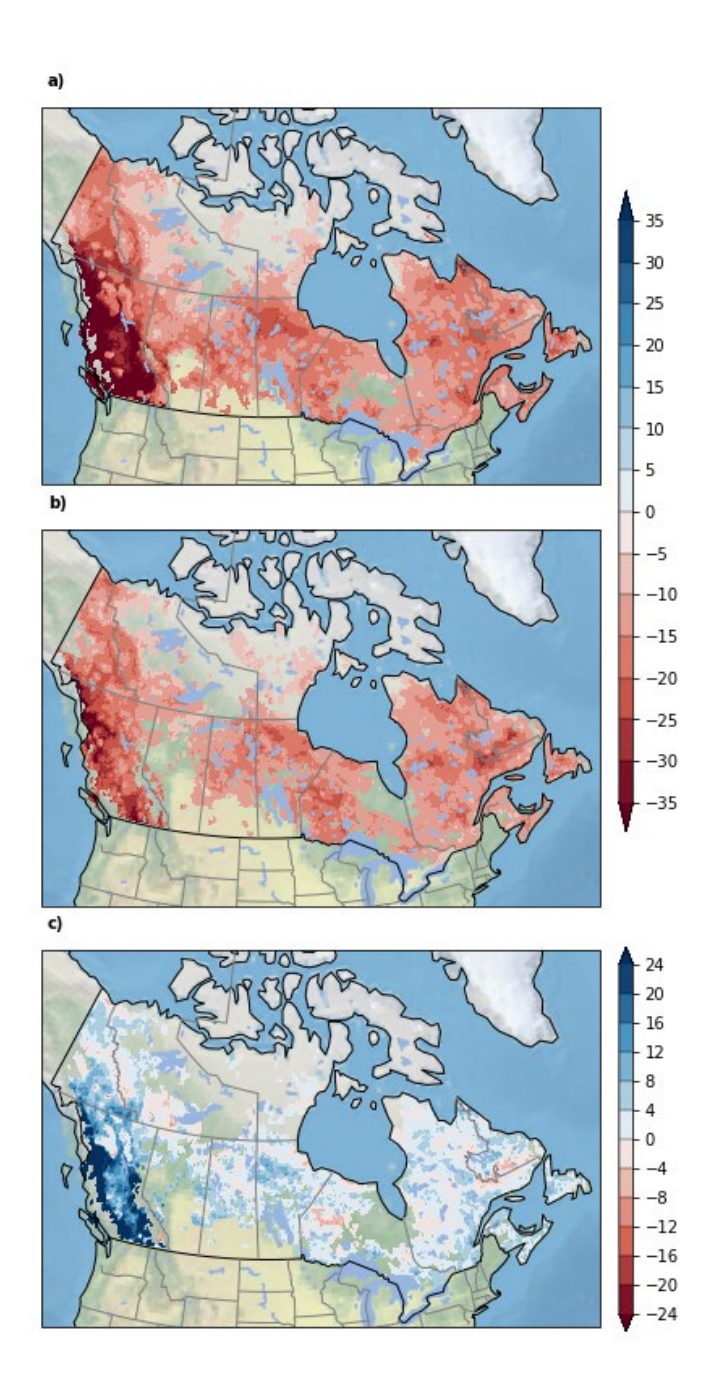




Figure B2: Trends for onset values (in days over 75 years) for a) "TS" method and b) "T" method, calculated over the whole-time window between 1950 and 2024, using ERA5 hourly reanalysis data. Differences between method "T" and method "TS" are shown in c). Trends are calculated using the Trend free Pre-Whitening method from the pyMannKendall library, with a statistical significance level of 0.95. Only significant trends are shown (i.e., for p-value < 0.05).

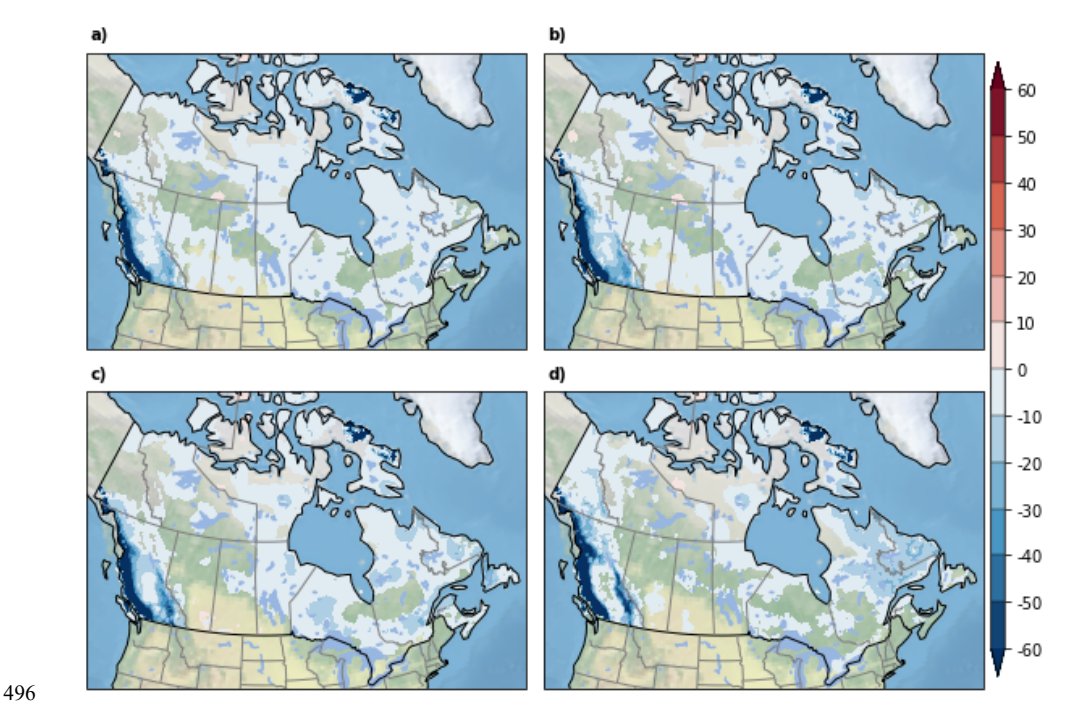


Figure B3: Trends for daily mean snow depth values (in cm over 75 years) on a) February 15th, b) March 15th, c) April 15th, and d) May 15th, calculated over the whole-time window between 1950 and 2024, using ERA5 hourly reanalysis data. Trends are calculated using the Trend free Pre-Whitening method from the *pyMannKendall* library, with a statistical significance level of 0.95. Only significant trends are shown (i.e., for p-value < 0.05).

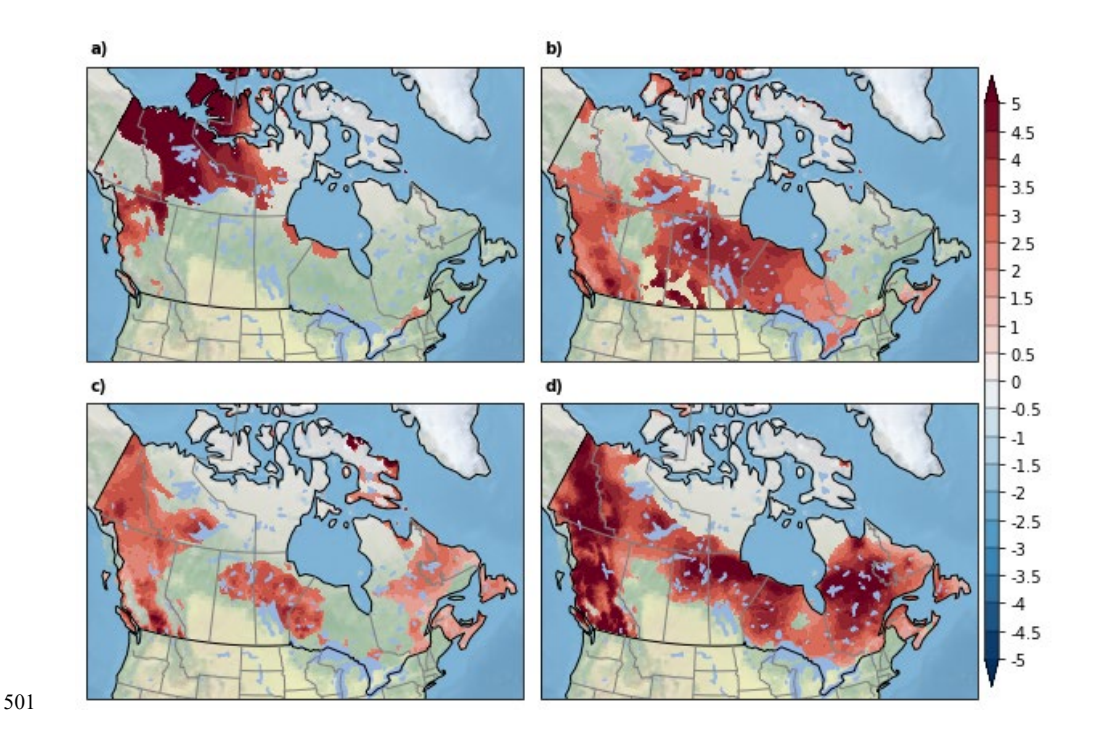


Figure B4: Trends for the monthly average values of daily maximum temperatures (in °C over 75 years) in a) February, b) March, c) April, and d) May, calculated over the whole-time window between 1950 and 2024, using ERA5 hourly reanalysis data. Trends are calculated using the Trend free Pre-Whitening method from the *pyMannKendall* library, with a statistical significance level of 0.95. Only significant trends are shown (i.e., for p-value < 0.05).



Appendix C - Overwintering of the Drought Code (DC)

Normal values (1991-2020) of the Drought Code value at the end of the fire season (DCf, Fig. C1) and of the winter precipitation (rw, Fig. C2), calculated between the local end of the fire season and the local onset date. Values are represented at a spatial resolution of approximately 31 km across Canada and were calculated using ERA5 reanalysis data.

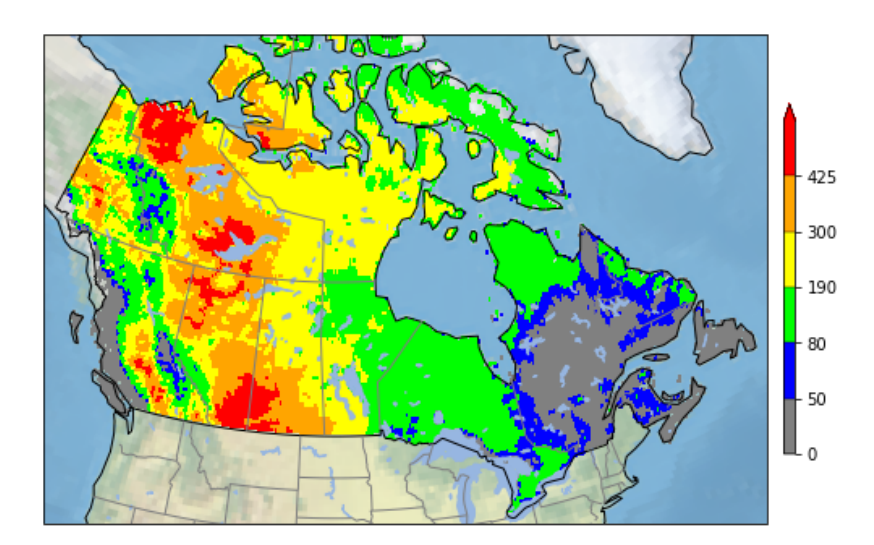


Figure C1: Climatology (1991-2020) of the Drought Code value at the end of the fire season (DCf) across Canada, calculated from each year locally, using the ERA5 hourly reanalysis data. All the areas except the ones in grey show an average DCf \geq 50, indicating where the overwinter adjustment of the DC typically apply, following Hanes and Wotton (2024)

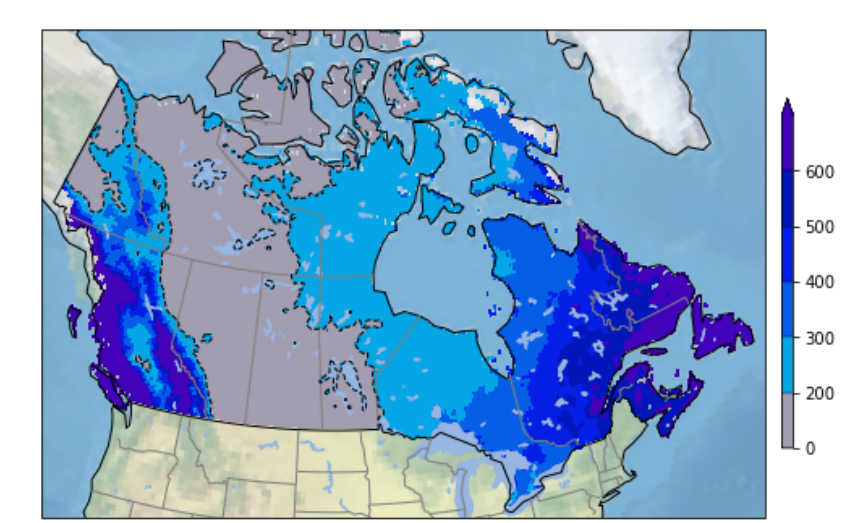




Figure C2: Climatology (1991-2020) of the winter precipitation (rw, in mm) across Canada, calculated from each year between the local end of the fire season and the local onset date, inclusively, using the ERA5 hourly reanalysis data. The black dashed contour line delineates areas where the average rw ≤ 200 mm, indicating where the overwinter adjustment of the DC typically applies, following Lawson and Armitage (2008).

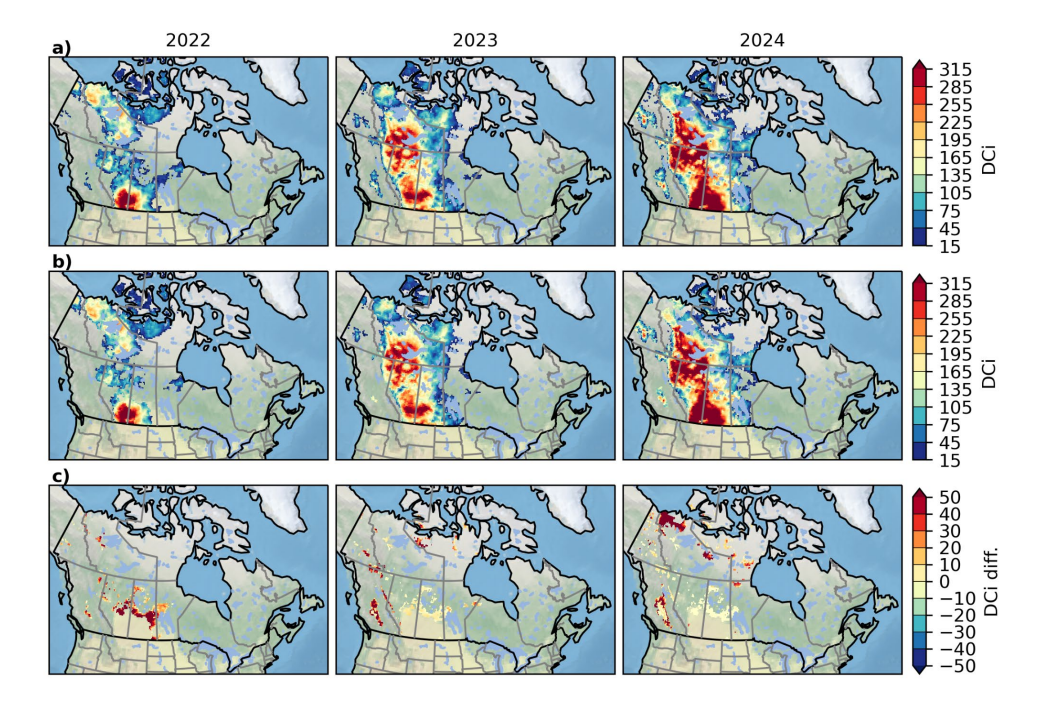


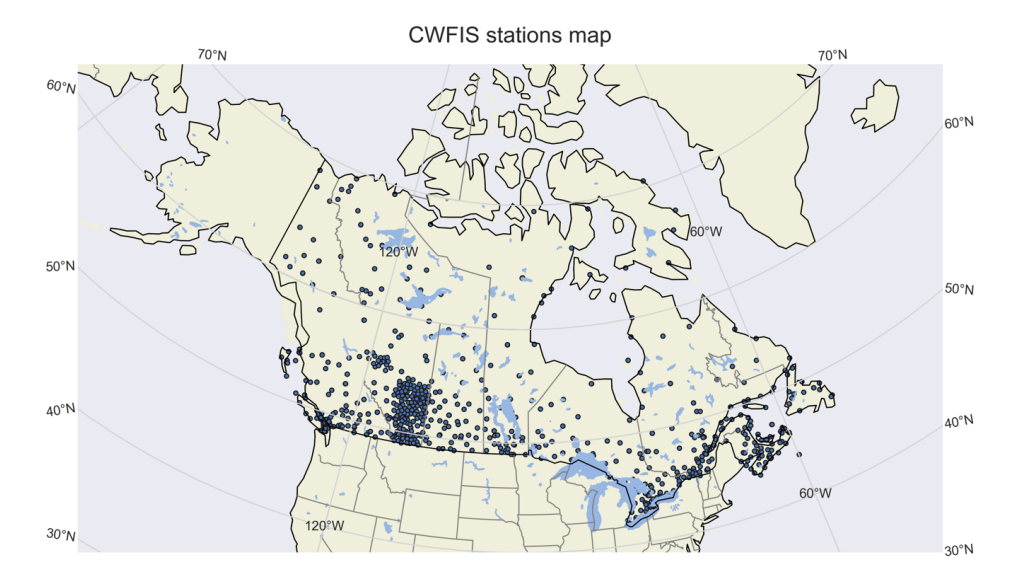
Figure C3: Comparison of overwintered start-up DC (DCi) values for years 2022, 2023 and 2024 when using a) last DC value from previous fall (DCf), or b) winter accumulated precipitation (WinterRain), for overwintering procedure application. Panels c) show the difference in DCi values between DCf and WinterRain methods, only where values are different. Overwintering adjustment applies when a) DCf \geq 50, and b) WinterRain \leq 200 mm, otherwise start-up default value of 15 is used.





Appendix D - FWI correlations with CWFIS stations observations

527528



529

Figure D1: Location of all stations in the CWFIS network that were used for comparing daily ERA5 FWI values obtained using both methods (solar noon and UTC).

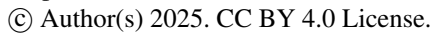






Table D1: Pearson correlation coefficients (p-value < 0.05) calculated between the daily CWFIS FWI, from the CWFIS meteorological stations across Canada (see their locations in Fig. D.1) and the daily FWI calculated using the ERA5 reanalysis data for both solar noon (SN) and classical UTC (UTC) methods, for each year from 2015 to 2024, and for each month from May to September, and considering all months (May-September). Average coefficients value for significant correlations only (p-value < 0.05) are given in parenthesis.

Year	May		June		July		August		September		All months	
	SN	UTC	SN	UTC	SN	UTC	SN	UTC	SN	UTC	SN	UTC
2015	0.79	0.79	0.75	0.75	0.75	0.75	0.74	0.75	0.81	0.81	0.77	0.77
	(0.82)	(0.82)	(0.77)	(0.77)	(0.76)	(0.76)	(0.76)	(0.76)	(0.83)	(0.83)	(0.79)	(0.79)
2016	0.85	0.86	0.75	0.75	0.71	0.71	0.75	0.75	0.80	0.79	0.77	0.77
	(0.88)	(0.88)	(0.77)	(0.77)	(0.73)	(0.72)	(0.76)	(0.76)	(0.81)	(0.81)	(0.79)	(0.79)
2017	0.81	0.80	0.78	0.78	0.70	0.70	0.75	0.75	0.83	0.82	0.77	0.77
	(0.85)	(0.85)	(0.80)	(0.80)	(0.72)	(0.72)	(0.77)	(0.77)	(0.83)	(0.83)	(0.79)	(0.79)
2018	0.80	0.80	0.79	0.79	0.75	0.75	0.73	0.73	0.78	0.78	0.77	0.77
	(0.82)	(0.82)	(0.80)	(0.80)	(0.76)	(0.76)	(0.74)	(0.75)	(0.81)	(0.81)	(0.79)	(0.79)
2019	0.79	0.80	0.77	0.77	0.73	0.73	0.74	0.74	0.76	0.76	0.76	0.76
	(0.83)	(0.83)	(0.80)	(0.80)	(0.74)	(0.75)	(0.75)	(0.75)	(0.78)	(0.77)	(0.78)	(0.78)
2020	0.79	0.80	0.76	0.76	0.74	0.74	0.75	0.75	0.75	0.75	0.76	0.76
	(0.82)	(0.82)	(0.79)	(0.78)	(0.76)	(0.75)	(0.76)	(0.76)	(0.77)	(78)	(0.78)	(0.78)
2021	0.78	0.79	0.82	0.82	0.74	0.74	0.78	0.78	0.78	0.78	0.78	0.78
	(0.82)	(0.82)	(0.83)	(0.83)	(0.76)	(0.76)	(0.80)	(0.80)	(0.80)	(0.80)	(0.80)	(0.80)
2022	0.78	0.76	0.79	0.79	0.77	0.76	0.75	0.75	0.80	0.80	0.78	0.77
	(0.82)	(0.82)	(0.81)	(0.81)	(0.78)	(0.78)	(0.77)	(0.77)	(0.82)	(0.82)	(0.80)	(0.80)
2023	0.83	0.83	0.80	0.79	0.70	0.70	0.78	0.78	0.81	0.81	0.78	0.78
	(0.85)	(0.85)	(0.80)	(0.81)	(0.72)	(0.72)	(0.78)	(0.78)	(0.82)	(0.82)	(0.80)	(0.80)
2024	0.79	0.79	0.81	0.81	0.78	0.78	0.78	0.78	0.82	0.82	0.80	0.80
	(0.82)	(0.82)	(0.82)	(0.82)	(0.79)	(0.79)	(0.79)	(0.79)	(0.83)	(0.83)	(0.81)	(0.81)
All	0.80	0.80	0.78	0.78	0.74	0.74	0.76	0.76	0.79	0.79	0.77	0.77
years	(0.83)	(0.83)	(0.80)	(0.80)	(0.75)	(0.75)	(0.77)	(0.77)	(0.81)	(0.81)	(0.79)	(0.79)



center is also strongly acknowledged.



538 **Author contribution** 539 JD developed the solar noon method as well as the Python code to run the model from gridded data and 540 performed the data comparison and validation. CB updated the Python code and generated the dataset. CB and 541 JD prepared the manuscript with contributions from all co-authors. All the authors contributed to the discussion 542 of the dataset and reviewed and edited the paper. 543 **Competing interests** 544 The authors declare that they have no conflict of interest. 545 Disclaimer 546 The authors declare that no funds, grants, or other support were received during the preparation of this 547 manuscript. 548 Acknowledgements 549 The authors would like to thank Natural Resources Canada (Canadian Forest Service) for the financial support of 550 this project at the ESCER center of UQAM. We would like to thank Fréderic Toupin from the department of Earth 551 and atmospheric sciences of UQAM for providing all the technical tools necessary for the successful completion 552 of the simulations, and his help with the web site development. Finally, we thank ECMWF for sharing the fifth-553 generation reanalysis data ERA5 (https://www.ecmwf.int/en/forecasts/datasets/reanalysis-datasets/era5). 554 This work was funded by Natural Resources of Canada (through Grant and Contribution program) and by 555 the Discovery Grant program and the Alliance program grant of the Natural Sciences and Engineering Research 556 Council of Canada (NSERC; i.e. #2022-05032) obtained by Pr. Philippe Gachon. Computations were made on the 557 supercomputers, managed by Calcul Québec and the Digital Research Alliance of Canada, whose operation is 558 funded by the Canada Foundation for Innovation, Ministère de l'Économie et de l'Innovation du Québec (MEI) 559 and the Fonds de recherche du Québec-Nature et technologies (FRQNT). The help of Katja Winger of the ESCER





- 561 References
- Barnes, C., Boulanger, Y., Keeping, T., Gachon, P., Gillett, N., Boucher, J., Roberge, F., Kew, S., Haas, O.,
- Heinrich, D., Vahlberg, M., Singh, R., Elbe, M., Sivanu, S., Arrighi, J., Van Aalst, M., Otto, F., Zachariah, M.,
- Krikken, F., et al.: Climate change more than doubled the likelihood of extreme fire weather conditions in
- eastern Canada, Scientific Report, http://dx.doi.org/10.25561/105981, 2023.
- 566 Baldwin, K., Allen, L., Basquill, S., Chapman, K., Downing, D., Flynn, N., MacKenzie, W., Major, M., Meades,
- 567 W., Meidinger, D., Morneau, C., Saucier, J-P., Thorpe, J., and Uhlig, P.: Vegetation Zones of Canada: a
- 568 Biogeoclimatic Perspective. [Map] Scale 1:5,000,000, Natural Resources Canada, Canadian Forest Service,
- 569 Great Lake Forestry Center, Sault Ste. Marie, ON, Canada, 2019.
- 570 Benoit, C., Demers, I., Roberge, F., Gachon, P., and Laprise, R.: Inondations des printemps 2017 et 2019 dans le
- 571 bassin versant de la rivière des Outaouais (Québec, Canada) : analyse des facteurs physiographiques et
- 572 météorologiques en cause, in: Les inondations au Québec : risques, aménagement du territoire, impacts
- 573 socioéconomiques et transformation des vulnérabilités, edited by: Buffin-Bélanger, T., Maltais D. and Gauthier,
- 574 M., Presse de l'Université du Québec, 29–58, 2022.
- 575 Boulanger, Y., Arseneault, D., Bélisle, A.C., Bergeron, Y., Boucher, J., Boucher, Y., Danneyrolles, V., Erni, S.,
- 576 Gachon, P., Girardin, M.P., Grant, E., Grondin, P., Jetté, J.P., Labadiem, G., Leblond, M., Leduc, A., Puigdevall,
- 577 J.P., St-Laurent, M.H., Tremblay, J.A., and Waldron, K.: The 2023 wildfire season in Québec: an overview of
- 578 extreme conditions, impacts, lessons learned and considerations for the future, Can. J. For. Res., 55, 1–21,
- 579 <u>http://dx.doi.org/10.1139/cjfr-2023-0298</u>, 2025.
- 580 Canadian Forest Fire Danger Rating System (CFFDRS), Natural Resources Canada website,
- 581 https://cwfis.cfs.nrcan.gc.ca/background/summary/fdr, last access: 19 August 2025.
- 582 Canadian Forest Service: Tables for the Canadian Forest Fire Weather Index System, 4th ed., Environ. Can.,
- 583 Can. For. Serv., Ottawa, Ont, For. Tech. Rep. 25, 48 pp., 1984.
- 584 Canadian Wildland Fire Information System (CWFIS): Data Sources and Methods. Natural Resources Canada.
- 585 https://cwfis.cfs.nrcan.gc.ca/background/dsm/fwi, n.d.
- 586 Copernicus Climate Change Service (C3S): ERA5 hourly data on single levels from 1940 to present, Climate Data
- 587 Store (CDS), https://cds.climate.copernicus.eu/datasets/reanalysis-era5-single-levels?tab=overview, last access:
- 588 19 August 2025.





- 589 Doblas-Reyes, F.J., Sörensson, A.A., Almazroui, M., Dosio, A., Gutowski, W.J., Haarsma, R., Hamdi, R.,
- 590 Hewitson, B., Kwon, W.-T., Lamptey, B.L., Maraun, D., Stephenson, T.S., Takayabu, I., Terray, L., Turner, A.,
- and Zuo, Z.: Linking Global to Regional Climate Change, in: Climate Change 2021: The Physical Science Basis.
- 592 Contribution of Working Group I to the Sixth Assessment Report of the Intergovernmental Panel on Climate
- 593 Change, edited by: Masson-Delmotte, V., Zhai, P., Pirani, A., Connors, S.L., Péan, C., Berger, S., Caud, N., Chen,
- 594 Y., Goldfarb, L., Gomis, M.I., Huang, M., Leitzell, K., Lonnoy, E., Matthews, J.B.R., Maycock, T.K., Waterfield,
- 595 T., Yelekçi, O., Yu, R., and Zhou, B., Cambridge University Press, Cambridge, United Kingdom and New York,
- 596 NY, USA, pp. 1363–1512, doi: 10.1017/9781009157896.012, 2021.
- 597 Duffie, J. A., Beckman, W. A., and Blair, N.: Solar Engineering of Thermal Processes, Photovoltaics and Wind,
- 598 Fifth Edition, John Wiley & Sons, Inc., https://doi.org/10.1002/9781119540328, 2020.
- 599 Environment and Climate Change Canada (ECCC). Canadian Climate Normals 1991–2020 Data DELINE,
- 600 NORTHWEST TERRITORIES, https://climate.weather.gc.ca/climate_normals/, last access: 5 June 2025.
- 601 de Groot, W. J., Goldammer, J. G., Keenan, T., Brady, M. A., Lynham, T. J., Justice, C. O., et al.: Developing a
- 602 global early warning system for wildland fire, For. Ecol. and Manag., 234(1),
- 603 https://doi.org/10.1016/j.foreco.2006.08.025, 2006.
- 604 Hanes, C., Wotton, M., Woolford, D. G., Martell, D. L., and Flannigan, M.: Preceding Fall Drought Conditions
- and Overwinter Precipitation Effects on Spring Wildland Fire Activity in Canada, Fire, 3(2), 24.
- 606 <u>https://doi.org/10.3390/fire3020024</u>, 2020.
- Hanes, C. and Wotton, M.: Updated guidance for the Drought Code overwintering adjustment, Can. Wildland
- 608 Fire Smoke Newsl., Can. Wildfire, 2-8, 2024.
- 609 Hebert, P.: Great Bear Lake, Northwest Territories, Encyclopedia of Earth, Washington, DC: Environmental
- 610 Information Coalition, National Council for Science and the Environment, Available at:
- 611 http://www.eoearth.org/view/article/51cbede97896bb431f694ac8/, last access: 7 December 2007.
- Hersbach, H., Bell, B., Berrisford, P., Hirahara, S., Horányi, A., Muñoz-Sabater, J., Nicolas, J., Peubey, C.,
- 613 Radu, R., Schepers, D., Simmons, A., Soci, C., Abdalla, S., Abellan, X., Balsamo, G., Bechtold, P., Biavati, P.,
- 614 Bidlot, J., Bonavita, M., De Chiara, G., Dahlgren, P., Dee, D., Diamantakis, M., Dragani, R., Flemming, J.,
- 615 Forbes, R., Fuentes, M., Geer, A., Haimberger, H., Healy, S., Hogan, R. J., Hólm, E., Janisková, M., Keeley, S.,
- 616 Laloyaux, P., Lopez, P., Lupu, C., Radnoti, G., de Rosnay, P., Rozum, I., Vamborg, F., Villaume, S., and
- Thépaut, J.-N.: The ERA5 global reanalysis, Q. J. Roy. Meteor. Soc., 146, 1999–2049,
- 618 https://doi.org/10.1002/qj.3803, 2020.





- 619 Intergovernmental Panel on Climate Change (IPCC): Climate Change 2021: The Physical Science Basis.
- 620 Contribution of Working Group I to the Sixth Assessment Report of the Intergovernmental Panel on Climate
- 621 Change [Masson-Delmotte, V., Zhai, P., Pirani, A., Connors, S.L., Péan, C., Berger, S., Caud, N., Chen, Y.,
- 622 Goldfarb, L., Gomis, M.I., Huang, M., Leitzell, K., Lonnoy, E., Matthews, J.B.R., Maycock, T.K., Waterfield,
- 623 T., Yelekçi, O., Yu, R., and Zhou, B. (eds.)], Cambridge University Press, Cambridge, United Kingdom and
- 624 New York, NY, USA, 2391 pp., doi:10.1017/9781009157896, 2021.
- 625 Jain P., Wang X., and Flannigan M. D.: Trend analysis of fire season length and extreme fire weather in North
- 626 America between 1979 and 2015, Int. J. Wildland Fire, 26, 1009–1020, https://doi.org/10.1071/WF17008, 2017.
- 627 Kouki, K., Luojus, K., and Riihelä, A.: Evaluation of snow cover properties in ERA5 and ERA5-Land with several
- 628 satellite-based datasets in the Northern Hemisphere in spring 1982–2018, The Cryosphere, 17(12), 5007–5026.
- 629 https://doi.org/10.5194/tc-17-5007-2023, 2023.
- 630 Lawson, B.D. and Armitage, O.B.: Weather Guide for the Canadian Forest Fire Danger Rating System, Nat. Res.
- 631 Can., Can. For. Serv., Edmonton, Alta., 84 pp., 2008.
- 632 Lei, Y., Pan, J., Xiong, C., Jiang, L., and Shi, J.: Snow depth and snow cover over the Tibetan Plateau observed
- 633 from space in against ERA5: matters of scale, Clim. Dynam., 60, 1523–1541, https://doi.org/10.1007/s00382-
- 634 022-06376-0, 2022.
- 635 Llerena, A., Gachon, P., and Laprise, R.: Precipitation Extremes and Their Links with Regional and Local
- Temperatures: A Case Study over the Ottawa River Basin, Canada, Atmosphere, 14(7), 1130.
- 637 http://dx.doi.org/10.3390/atmos14071130, 2023.
- 638 Muñoz-Sabater, J., Dutra, E., Agustí-Panareda, A., Albergel, C., Arduini, G., Balsamo, G., Boussetta, S.,
- 639 Choulga, M., Harrigan, S., Hersbach, H., Martens, B., Miralles, D. G., Piles, M., Rodríguez-Fernández, N. J.,
- 640 Zsoter, E., Buontempo, C., and Thépaut, J.-N.: ERA5-Land: A state-of-the-art global reanalysis dataset for land
- applications, Earth Syst. Sci. Data, 13, 4349–4383, https://doi.org/10.5194/essd-13-4349-2021, 2021.
- 642 Natural Resources Canada: Hydrographic Features CanVec Series 1M, Government of Canada [data set],
- 643 <u>https://open.canada.ca/data/en/dataset/9d96e8c9-22fe-4ad2-b5e8-94a6991b744b.</u>
- Python Package Index PyPI: daylight 0.1.3 [code]. https://pypi.org/project/daylight/, 2020.
- 645 Roberge, F., Di Luca, A., Laprise, R., Lucas-Picher, P., and Thériault, J.: Spatial spin-up of precipitation in
- 646 limited-area convection-permitting simulations over north america using the crcm6/gem5.0 model, Geosci.
- 647 Model Dev., 17(4), 1497–1510, 2024.





- 648 Sjöström, J., Vermina Plathner, F., and Granström, A.: 70 Years of observational weather data show increasing
- 649 fire danger for boreal Europe and reveal bias of ERA5 reanalysed data, Sci. Rep., 15(1), 20111.
- 650 https://doi.org/10.1038/s41598-025-04200-3, 2025.
- Turner, J.A. and Lawson, B.D.: Weather in the Canadian Forest Fire Danger Rating System, A user guide to
- 652 national standards and practices, Environment Canada, Pacific Forest Research Centre, Victoria, BC. BC-X-177,
- 653 1978.
- 654 Van Wagner, C.E. and Pickett, T.L.: Equations and FORTRAN program for the Canadian Forest Fire Weather
- 655 Index System, Canadian Forestry Service, Petawawa National Forestry Institute, Chalk River, Ontario, Forestry
- 656 Technical Report 33, 18 p, 1985.
- 657 Van Wagner, C.: Development and structure of the Canadian Forest Fire Weather Index System, Paper presented
- at the Can. For. Serv., Forestry Tech. Rep., https://ostrnrcan-dostrncan.canada.ca/handle/1845/228434, 1987.
- 659 Vitolo, C., Di Giuseppe, F., Barnard, C., Coughlan, R., San-Miguel-Ayanz, J., Libertá, G., and Krzeminski, B.:
- 660 ERA5-based global meteorological wildfire danger maps, Scientific Data, 7, 216,
- 661 https://doi.org/10.1038/s41597-020-0554-z, 2020.
- 662 Wang, X., Thompson, D., Marshall, G., Tymstra, C., Carr, R., and Flannigan, M.: Increasing frequency of
- extreme fire weather in Canada with climate change, Clim. Change, 130, 573–586,
- https://doi.org/10.1007/s10584-015-1375-5, 2015.
- Wang, X., Cantin, A., Parisien, M.-A., Wotton, M., Anderson, K., Moore, B., Schiks, T., and Flannigan, M.:
- 666 Canadian Forest Fire Danger Rating System, v1.9.0, https://r-forge.r-project.org/projects/cffdrs/, 2024.
- 667 Wotton, B.M. and Flannigan, M.D.: Length of the fire season in a changing climate, For.Chron., 69, 187-192,
- 668 https://doi.org/10.5558/tfc69187-2, 1993.